To further verify the applicability of this technique, we have also compared the extensive experimental data of Haydl *et al.* [7, 8] with our model; in all cases excellent agreement has been obtained. Fig. 3 shows a comparison of some of their measurements and our calculations over a wide range of CPW

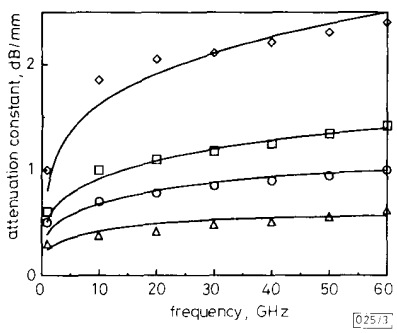

Fig. 3 *Comparison between this model and experimental results of Reference 8*

CPW dimensions:
◇ $a = 2\,\mu m$, $b = 15\,\mu m$, and $t = 0{\cdot}25\,\mu m$
□ $a = 2\,\mu m$, $b = 15\,\mu m$, and $t = 0{\cdot}5\,\mu m$
○ $a = 6\,\mu m$, $b = 45\,\mu m$, and $t = 0{\cdot}25\,\mu m$
△ $a = 6\,\mu m$, $b = 45\,\mu m$, and $t = 0{\cdot}5\,\mu m$
——— from conformal map calculation
Open symbols: experimental results

dimensions. Again, no fitting factors are used; only the dimensions of the CPW and conductivity of the metal are required for the calculation. In summary, we have demonstrated a quasistatic technique for the calculation of conductor loss in CPW which shows excellent agreement with experimental measurements. The technique is numerically efficient, and can be readily applied to other planar transmission line structures.

Acknowledgments: This work was sponsored in part by the Joint Services Electronics Program under grant number AFOSR 49620-89-C-0044, and by the Advanced Research Projects Agency Application Specific Electronic Modules program.

© IEE 1993
12th May 1993

M. S. Islam, E. Tuncer and D. P. Neikirk (*Department of Electrical & Computer Engineering, The University of Texas at Austin, Austin, Texas 78712, USA*)

References

1 RAMO, S., WHINNERY, J. R., and DUZER, VAN T.: 'Fields and waves in communication electronics' (Wiley, New York, 1984), 2nd edn.
2 WEN, C. P.: 'Coplanar waveguide: A surface strip transmission line suitable for nonreciprocal gyromagnetic device applications', *IEEE Trans.*, 1969, **MTT-17,** (12), pp. 1087–1088
3 WENTWORTH, S. M., NEIKIRK, D. P., and BRAHCE, C. R.: 'The high frequency characteristics of tape automated bonding (TAB) interconnects', *IEEE Trans.*, 1989, **CHMT-12,** (3), pp. 340–347
4 WHEELER, H.: 'Transmission-line properties of a strip on a dielectric sheet on a plane', *IEEE Trans.*, 1977, **MTT-25,** pp. 631–647
5 GUPTA, K. C., GARG, R., and BAHL, I. J.: 'Microstrip lines and slotlines' (Artech House Inc., Norwood, MA, 1979), p. 287
6 COLLIN, R. E.: 'Foundations for microwave engineering' (McGraw-Hill, New York, 1992), 2nd edn., pp. 898–910
7 HAYDL, W. H., BRAUNSTEIN, J., KITAZAWA, T., SCHLECHTWEG, M., TASKER, P., and EASTMAN, L. F.: 'Attenuation of millimeterwave coplanar lines on gallium arsenide and indium phosphide over the range of 1–60 GHz'. IEEE MTT-S Int. Microwave Symp. Dig., June 1991, pp. 349–352
8 HAYDL, W. H.: 'Experimentally observed frequency variation of the attenuation of millimeterwave coplanar transmission lines with thin metallization', *IEEE Microw. & Guided Wave Lett.*, 1992, **2,** (8), pp. 322–324

HIGH PRESSURE H_2 LOADING AS A TECHNIQUE FOR ACHIEVING ULTRAHIGH UV PHOTOSENSITIVITY AND THERMAL SENSITIVITY IN GeO_2 DOPED OPTICAL FIBRES

P. J. Lemaire, R. M. Atkins, V. Mizrahi and W. A. Reed

Indexing terms: Optical fibres, Photorefractive materials

High pressure 'hydrogen loading' has been used to sensitise standard singlemode fibres, resulting in the largest reported UV induced index changes for low GeO_2 fibres. Grating bandwidths of 4 nm and peak Δns of $5{\cdot}9 \times 10^{-3}$ have been reproducibly achieved. Substantial index changes have also been achieved by rapidly heating H_2 loaded fibres of various compositions.

Introduction: There is widespread interest in the technology used for the UV writing of phase gratings in optical fibres [1]. Grating formation is generally dependent on the existence of Ge related defects which can vary significantly from fibre to fibre. Nevertheless index changes of $1{\cdot}2 \times 10^{-3}$ have been reported for low GeO_2 fibres in one study [2]. Alternatively, it has recently been shown that strong gratings can be formed in a single intense excimer laser pulse, by inducing physical damage in certain fibre types [3]. In general, however, it has not been possible to cause large and reproducible index changes in an arbitrarily chosen fibre. Typically, UV induced index changes have been limited to $\sim 3 \times 10^{-5}$ for standard singlemode fibres doped with 3% germania ($\Delta \simeq 3 \times 10^{-3}$) [4]. Enhancing the fibre photosensitivity has generally required increasing the GeO_2 doping level [4] or subjecting the fibre or preform [5, 6] to reducing conditions at high temperatures. Nonetheless the resultant peak index changes have usually been about 5×10^{-4} or less [4].

We report a simple technique which can sensitise fibres using a low temperature hydrogen treatment prior to the UV exposure. This hydrogen 'loading' is carried out by diffusing H_2 molecules into fibres at low temperatures and high pressures. Subsequent exposure to UV or intense heat (e.g. a flame or a CO_2 laser) causes the dissolved H_2 to react in the glass, typically at Ge sites, resulting in large permanent index changes in the fibre core. This technique has shown itself to be applicable to any GeO_2 doped fibre, and does not require the use of fibres made with high dopant levels or other special processing techniques.

Experiments: Standard singlemode fibres were exposed to high pressure hydrogen gas at temperatures ranging from ~ 21 to 75°C. Hydrogen pressures ranged from ~ 20 atm to over 750 atm. Treatment times were sufficient to achieve at least 95% of the equilibrium solubility at the fibre core. For 125 μm fibres a 12 day treatment at 21°C resulted in an H_2 solubility of ~ 116 *ppm*/atm [7, 8] (1 *ppm* is defined as 10^{-6} moles of H_2 per mole of SiO_2). Although shorter exposure times were possible at higher temperatures, it was desirable to avoid temperatures greater than ~ 100°C because these could cause overall fibre loss increases due to hydrogen reactions [7]. In addition, the solubility of H_2 in silica is proportional to $\exp(8{\cdot}67\,kJ/mole/RT)$, resulting in lower solubilities at higher temperatures. Typical H_2 concentrations that were used ranged from $\sim 2300\,ppm$ to $8{\cdot}5 \times 10^4\,ppm$, depending on the desired index changes. The H_2 concentration in the fibre core could be independently verified using the 1·24 μm H_2 first overtone absorption [7].

A standard AT&T MCVD singlemode fibre, with a core GeO_2 level of $\sim 3\%$, was loaded with 3·3% H_2. A 5 mm long grating (FWHM) was then formed by the UV side-writing technique [9] using 241 nm radiation at 30 Hz with a fluence of $\sim 300\,mJ/cm^2$ for 10 min. The transmission spectrum for the resultant grating had a spectral width of 4 nm (FWHM), as shown in Fig. 1. The peak-to-peak index change (Δn) is estimated to be $5{\cdot}9 \times 10^{-3}$, assuming a sinusoidal index modulation with no index changes at the minima of the inter-

ference pattern. This is the largest index change reported to date for a fibre having such a low GeO_2 content. The refractive index profile at the midpoint of a similar grating was measured using a York fibre profiler and was compared to an untreated fibre (Fig. 2). The space average core index had increased by $\sim 3{\cdot}4 \times 10^{-3}$. Similar bandwidths and index changes have been obtained using other standard MCVD and VAD fibres with cores doped with $\sim 3\%$ GeO_2.

Fig. 3 shows the UV induced loss changes that occurred on writing a strong grating in a 9% GeO_2 fibre that had been loaded with 4·1% H_2. The spectrum shows a strong short

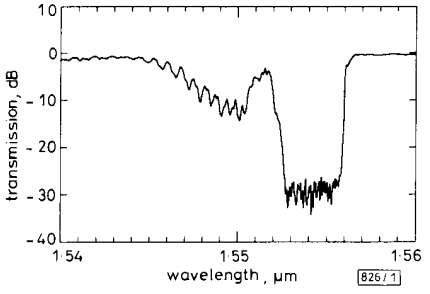

Fig. 1 *Transmission spectrum for ultrastrong grating written in standard singlemode fibre that was loaded with 3·3% H_2 prior to UV exposure*

Grating width is 3·96 nm (FWHM); features from 1·546 to 1·551 μm are due to radiation mode coupling

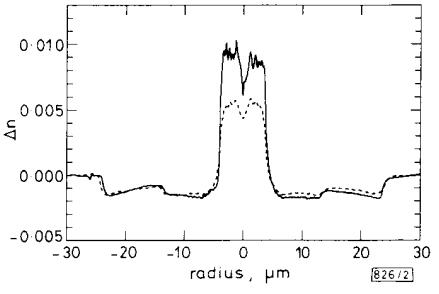

Fig. 2 *Refractive index profiles for a standard singlemode fibre with 3% GeO_2, and for a grating that was UV written in the same fibre after loading with 3·3% H_2*

Δn refers to index with respect to undoped silica
– – – – 3% GeO_2
——— after loading with 3·3% H_2

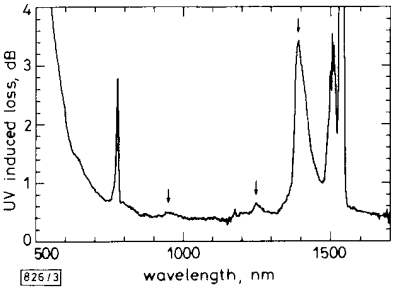

Fig. 3 *UV induced losses in ~5 mm long grating in fibre with 9% GeO_2*

Features at 770 and 1500 nm are due to the grating; marked peaks at 0·95, 1·24 and 1·39 μm are due to OH; loss accuracy is $\sim \pm 0{\cdot}1$ dB

wavelength edge and a prominent Si–OH absorption at 1·39 μm. The concentration of OH can be estimated to be ~8·4 mol%, quite similar to the GeO_2 content of the fibre. A similar spectrum for a 3% GeO_2 fibre containing 1·4% H_2 showed ~2·9% OH and a proportionally lower short wavelength edge.

It was interesting to determine if large index changes could be induced in the H_2 loaded fibres by means other than UV exposure. A 3% GeO_2 fibre was loaded with 4·3% H_2 and then was rapidly heated (< 1 s) over a 62 mm length using a miniature gas–oxygen torch with a flame size of ~3 mm. Loss changes were monitored from 0·4 to 1·7 μm and the growth of a prominent OH peak was noted, corresponding to the formation of ~2·9% of Si–OH. As had been seen in UV written gratings the OH level was the same as the GeO_2 content of the fibre. By measuring fibre spectra in the deep UV region [10] it was determined that a strong 242 nm band grew in proportion to the OH increases in flame heated fibres. The presence of this 242 nm band indicated the formation of a large number of oxygen deficient GE sites. Another flame heating experiment was carried out using a 9% GeO_2 fibre that had been loaded with 1·8% H_2. The heating induced index increases (Δn) were 0·006 in the GeO_2 doped core. Index increases of 0·001 were seen in the phosphorus–fluorine doped cladding of the same fibre. Heating induced index increases of 0·002 and 0·003 have been achieved in H_2 loaded fibres with phosphosilicate and alumino-phosphosilicate cores, repectively.

Discussion: This hydrogen technique is distinguished from previous techniques [4–6] by the extremely large index changes that have been achieved, and by the fact that the H_2 is introduced inertly into the fibre at low temperatures. Subsequent exposure to UV irradiation or thermal energy then causes a reaction that leads to very large localised index increases, e.g. in the formation of a grating. The unreacted H_2 in the other sections of the fibre can then be outgassed. The only permanent changes are in the regions that were heated or UV irradiated. Unlike other techniques that rely on defect sites that are normally present at low concentrations, the present technique is capable of causing index-raising at *every* Ge site in the glass, thus leading to very large increases in index. The UV induced index changes are not affected by subtleties of fibre or preform processing, but rather are functions of the GeO_2 and H_2 concentrations and the UV exposure conditions. The index changes that have been achieved are sufficiently large that UV light could be used to pattern a guiding structure in H_2 loaded germanosilicate glass, for instance to write a waveguide core in a planar structure. A proposed model for the reaction in GeO_2 doped glasses is that H_2 molecules react at normal Si–O–Ge sites, resulting in the formation of Si–OH and oxygen deficient Ge defects, both of which contribute to the observed index changes. Preliminary experiments have shown that a substantial portion of the UV induced refractive index can be expected to be thermally stable at normal conditions [11]. This is consistent with general observations that OH defects tend to be stable in silicate materials at room temperature.

Conclusions: The largest UV induced index changes reported to date for standard GeO_2 doped telecommunication fibres have been achieved using H_2 'loaded' fibres. H_2 molecules are diffused into fibres at high pressure, and then made to react by the use of UV light or a rapid thermal treatment. Substantial index changes have also been achieved by the rapid heating of H_2 loaded fibres based on germanosilicate, phosphosilicate, and alumino-phosphosilicate glass compositions.

© IEE 1993
23rd April 1993

P. J. Lemaire, R. M. Atkins, V. Mizrahi and W. A. Reed (*AT&T Bell Laboratories, 600 Mountain Avenue, Murray Hill, New Jersey, 07974, USA*)

References

1 MIZRAHI, V.: 'Components and devices for optical communications based on UV-written-fiber phase gratings'. Proc. Conf. on Optical Fiber Communications, OFC '93, 1993, pp. 243–244
2 LIMBERGER, H. G., FONJALLAZ, P. Y., and SALATHÉ, R. P.: 'Spectral characterisation of photoinduced high efficient Bragg gratings in standard telecommunication fibres', *Electron. Lett.*, 1993, **29**, (1), pp. 47–48
3 ARCHAMBAULT, J.-L., REEKIE, L., and RUSSELL, P. ST. J.: '100% reflectivity Bragg reflectors produced in optical fibres by single excimer laser pulses', *Electron. Lett.*, 1993, **29**, (5), pp. 453–455

4 WILLIAMS, D. L., AINSLIE, B. J., ARMITAGE, J. R., and KASHYAP, R.: 'Enhanced photosensitivity in germania doped silica fibers for future optical networks'. Proc. European Conf. on Optical Communication, ECOC '92, 1992, pp. 425–428
5 ATKINS, R. M., NELSON, K. T., and WALKER, K. L.: 'Photorefractive optical fiber'. US Patent 5157747, 1992
6 OUELLETTE, F., GAGNON, D., and POIRIER, M.: 'Permanent photoinduced birefringence in a Ge-doped fiber', *Appl. Phys. Lett.*, 1991, **58**, (17), pp. 1813–1815
7 LEMAIRE, P. J.: 'Reliability of optical fibers exposed to hydrogen: prediction of long-term loss increases', *Opt. Eng.*, 1991, **30**, (6), pp. 780–789
8 SHACKELFORD, J. F., STUDT, P. L., and FULRATH, R. M.: 'Solubility of gases in glass: II: He, Ne, and H_2 in fused silica', *J. Appl. Phys.*, 1972, **43**, (4), pp. 1619–1626
9 MELTZ, G., MOREY, W. W., and GLENN, W. H.: 'Formation of Bragg gratings in optical fibers by a transverse holographic method', *Opt. Lett.*, 1989, **14**, (15), pp. 823–825
10 ATKINS, R. M.: 'Measurement of the ultraviolet absorption spectrum of optical fibers', *Opt. Lett.*, 1992, **17**, pp. 469–471
11 LEMAIRE, P. J., MIZRAHI, V., ATKINS, R. M., and KRANZ, K. S.: 'High-temperature stability of phase gratings in GeO_2-doped optical fibers'. Tech. Dig. Conf. Optical Fiber Commun., OFC '93, pp. 242–243

RACE-TRACK FLUXGATE GRADIOMETER

P. Ripka, K. Draxler and P. Kaspar

Indexing terms: Measurement, Magnetic fields

A fluxgate sensor with amorphous race-track (oval) core is described. The sensor measures DC magnetic field and magnetic field gradient simultaneously. The noise RMS values are 10 pT and 10 pT/cm, respectively, both in the 20 MHz–10 Hz frequency range.

The most popular ring-core fluxgate sensors have rather low sensitivity due to the strong demagnetisation [1]. If the gradiometric measurements are required, a system consisting of two separate sensors has to be used. In such a case the minimum obtainable gradiometric base is ~10 cm. A fluxgate magnetometer using 7 cm long oval-shape core etched from low-magnetostriction amorphous cobalt-based material was described recently [2]. A similar sensor allowing the simultaneous measurement of the DC magnetic field and gradient is presented here. The idea of using a single-core fluxgate for gradiometric measurement probably comes from Berkman [3]. The race-track sensor uses the advantages of the highly homogeneous magnetically-closed core with low demagnetisation. The sensing coil system is similar to that of the magnetoelastic sensor described in Reference 4, but the present sensor uses near-zero magnetostriction core material and purely conventional fluxgate principle leading to lower noise levels.

The sensor is shown in Fig. 1. The race-track core made from eight sheets, each 30 μm thick, is placed inside the plastic bobbin and wound by 300 turns of 0·3 mm excitation winding. The sensor is excited by the circuits described in Reference 5. The excitation frequency is 15 kHz, and peak–peak amplitude of the current 1·5 A. The power lost in the excitation is ~300 mW.

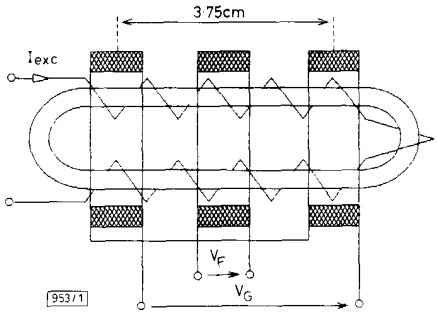

Fig. 1 *Fluxgate gradiometer showing oval-shape sensor core, excitation winding (I_{EXC}), central field measuring coil (V_F) and gradiometric coil pair (V_G)*

The sensing coil system consists of the centrally located 10 mm long field coil of 1000 turns; the gradiometric coil pair has 2 × 900 turns connected antiserially, each coil being divided into three 1 mm spaced sections of 300 turns to lower the coil capacitance. The coil length was 14 mm, the distance between the gradiometric coil centres giving the gradiometric base was 3·75 cm. The gradiometric coil pair was balanced using an adjustable extra turn to minimise the sensitivity to the homogeneous field component.

The sensor was calibrated using a 52 cm diameter Helmholtz coil pair. For the homogeneous field, the two 112 turns coils were connected serially, and the calibration current was 260 μA for 100 nT step; for the first gradient calibration the coils were connected antiserially, and the calibration current was 558 μA for the 10 nT/cm step.

The sensor output voltage was measured using a PAR 5210 lock-in amplifier: the internal filter was switched to the bandpass tracking mode, and the phase shift was adjusted to the maximum sensitivity. The measured sensitivities were 130 μV/nT for the homogeneous field, and 270 μV/nT cm^{-1} for the field gradient.

The residual sensitivity of the gradient coil to the homogeneous field component was 0·4 μV/nT. The sensor output to the 10 nT/cm calibration step is shown in Fig. 2. The noise

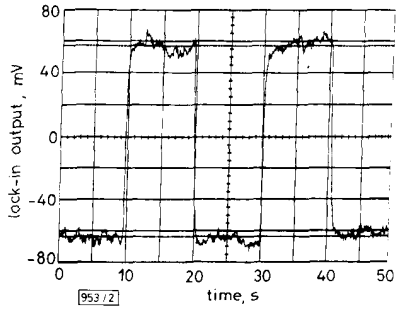

Fig. 2 *Response to 10 nT/cm gradient step (measured in normal laboratory environment)*
Sensitivity at output of lock-in amplifier was 12 mV/nT cm^{-1}

level is primarily due to the magnetic field laboratory noise converted into a gradient by the effect of near ferromagnetic bodies, and also by gradient noise from near-field sources.

The sensor noise was measured inside the six-layer permalloy shielding. The residual field in the sensor location was below 2 nT. The RMS noise values measured in the time domain were 10 pT for the field coil and 31 pT/cm for the gradient coil typically; in the 20 MHz–10 Hz frequency range, the peak-to-peak values were approximately 50 pT and 150 pT/cm respectively. The spectral properties of the sensor noise were measured using the noise analysis system described

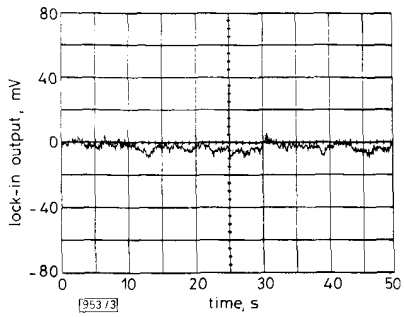

Fig. 3 *Gradient sensor noise (measured in the magnetic shielding)*
Sensitivity is same as in Fig. 2